

Initial Excited-State Relaxation of the Isolated 11-*cis* Protonated Schiff Base of Retinal: Evidence for in-Plane Motion from ab Initio Quantum Chemical Simulation of the Resonance Raman Spectrum

Marco Garavelli, Fabrizia Negri,* and Massimo Olivucci*[‡]

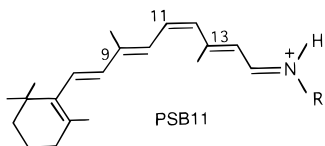
Dipartimento di Chimica “G. Ciamician”, Via F. Selmi, 2 Università di Bologna, I-40126 Bologna, Italy

Received May 18, 1998. Revised Manuscript Received November 9, 1998

Abstract: The intensity distribution in the resonance Raman (RR) spectrum of the 11-*cis* protonated Schiff base of retinal (PSB11) is modeled for the first time on the basis of ab initio quantum chemical calculations. To adequately represent the structure of PSB11, 4-*cis*- γ,η -dimethyl-C₉H₉ NH₂⁺ is chosen as a model. The RR spectra of the model PSB11 and of several isotopomers are compared with the experimental spectra of PSB11 in solution. An excellent agreement is obtained in the structurally sensitive fingerprint region of the spectra (1100–1300 cm⁻¹), where most of the observed details are quantitatively reproduced by the simulations. The 900–1100-cm⁻¹ region of the RR spectrum of PSB11, which contains the signatures of the S₀,S₁ potential energy changes due to the protein environment, is also well reproduced. On the basis of the simulations, it is concluded that the activity observed at ca. 970 cm⁻¹ in the spectrum of PSB11 in solution is due to in-plane modes, while a superposition of in-plane and out-of-plane motions is responsible for the increased RR activity in rhodopsin. The present analysis of RR activities along with the computed relaxation path structure provides support for the interpretation of the initial relaxation of photoexcited PSB11 in solution in terms of initial in-plane motion out of the Franck–Condon region followed by slow out-of-plane (i.e., *cis* → *trans* torsional) evolution along a flat energy plateau. Furthermore, the quality of the simulated spectra suggests that the quantum chemical method used in this work can be employed quantitatively to assist in the characterization of photoreaction intermediates in the visual cycle.

1. Introduction

The 11-*cis*-retinal protonated Schiff base (PSB11) is the chromophore of the protein rhodopsin, the human retina visual pigment. The photoisomerization of PSB11 to its *all-trans* isomer (PSBT) is one of the fastest chemical reactions observed so far.¹



Recently, femtosecond pump–probe experiments have shed light on the ultrafast excited-state dynamics of PSB11 both in the protein cavity and in solution. In particular, it has been shown that photoexcitation of PSB11 in rhodopsin yields a transient fluorescent state (FS) with a lifetime of 50–60 fs.^{2,3} After this state is left, ground-state PSBT is formed within 200 fs.⁴ In contrast, the photochemistry of free PSB11 in solution

is almost 2 orders of magnitude slower: in methanol, PSB11 has a ca. 3-ps fluorescence lifetime, and PSBT is formed in 10 ps.⁵ Before femtosecond experiments were available, resonance Raman (RR) spectroscopy, a powerful tool to study the early stages of excited-state dynamics, was extensively employed both to identify photoreaction intermediates^{6,7} and to investigate the initial dynamics of the primary light-induced events in rhodopsin.⁸ In these studies, the effect of the protein environment was identified in an enhanced torsional activity by comparing the RR response of PSB11 in solution and in the protein.⁹

The understanding of the production and decay of the transient FS in terms of the evolution of the PSB11 molecular structure on the excited state is a major objective of the investigation of the photoisomerization mechanism and, ultimately, of the catalytic effect of the protein environment. In principle, this understanding would be possible on the basis of the result of quantum or semiclassical dynamics computations based upon an accurate ab initio quantum chemical force field. Regrettably, such computations are still unpracticable for a molecule of the size of PSB11. On the other hand, information on the dynamics may be derived by investigating the fine structure of the force field which controls the molecular motion. The structure of this force field also determines the intensity distribution in the RR spectrum. In this regard, a reliable model must be able to account

* Corresponding authors.

[‡] Present address: Istituto di Chimica Organica, Pian dei Mantellini 44, Università di Siena, I-53100 Siena, Italy.

(1) Yoshizawa, T.; Kuwata, O. In *CRC Handbook of Organic Photochemistry and Photobiology*; Horspool, W. M., Song, P.-S., Eds.; CRC Press: Boca Raton, FL, 1995, 1493–1499.

(2) Kochendoerfer, G. G.; Mathies, R. A. *J. Phys. Chem.* **1996**, *100*, 14526–14532.

(3) Kandori, H.; Sasabe, H.; Nakanishi, K.; Yoshizawa, T.; Mizukami, T.; Shichida Y. *J. Am. Chem. Soc.* **1996**, *118*, 1002–1005.

(4) (a) Schoenlein, R. W.; Peteanu, L. A.; Mathies, R. A.; Shank, C. V. *Science* **1991**, *254*, 412–415. (b) Wang, Q.; Schoenlein, R. W.; Peteanu, L. A.; Mathies, R. A.; Shank, C. V. *Science* **1994**, *266*, 422–424.

(5) Kandori, H.; Katsuta, Y.; Ito, M.; Sasabe, H. *J. Am. Chem. Soc.* **1995**, *117*, 2669–2670.

(6) Oseroff, A. R.; Callender, R. H. *Biochemistry* **1974**, *13*, 4243–4248.

(7) Callender, R.; Honig, B. *Annu. Rev. Biophys. Bioeng.* **1977**, 33–55.

(8) Loppnow, G. R.; Mathies, R. A. *Biophys. J.* **1988**, *54*, 35–43.

(9) Palings, I.; Pardo, J. A.; van den Berg, E.; Winkel, C.; Lugtenburg, J.; Mathies, R. A. *Biochemistry* **1987**, *26*, 2544–2556.

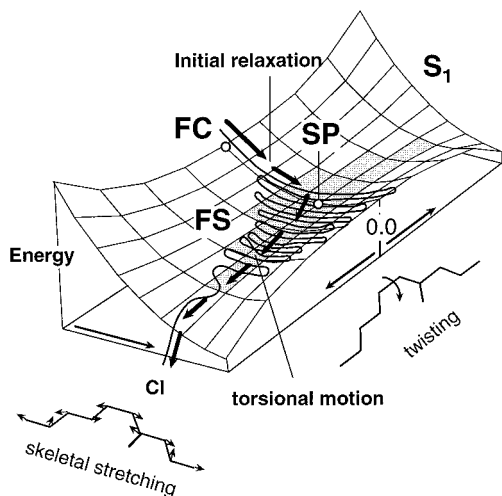
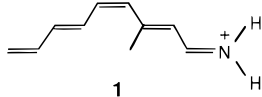


Figure 1. Structure of the S_1 energy surface along the relaxation path of the PSB11 model **1**. The stream of arrows indicate the relaxation path. SP indicates the fully relaxed planar stationary point (a very flat energy minimum). (Notice that the initial part of the path corresponds to a valley connecting FC to SP. As discussed in the text, this valley becomes very flat when approaching point SP.) The full line represents a hypothetical classical trajectory released near FC with a small initial torsional perturbation. The shaded area corresponds to the picosecond transient fluorescent state (FS) discussed in the text. Notice that FS corresponds to an energy plateau.

simultaneously for the combined information available from RR spectroscopy and femtosecond studies.

Recently, we have investigated the S_1 energy surface of the realistic PSB11 model 4-*cis*- γ -methylnona-2,4,6,8-tetraeniminium cation (**1**) by means of high-level ab initio quantum chemical computations¹⁰ and a minimum energy path (MEP) search. We have found that, in isolated conditions, **1** has a planar



ground-state structure. Photoexcitation of this structure to its first excited state (S_1) initiates relaxation along the energy surface shown in Figure 1. Accordingly, the excited-state motion must occur along an almost barrierless path (see arrows) which connects the Franck–Condon (FC) structure to a low-lying S_1/S_0 conical intersection (CI) from which photoproducts are formed. The corresponding reaction coordinate indicates that initial acceleration out of the FC region is dominated by skeletal relaxation and has no component along the torsional or other out-of-plane coordinates. On the other hand, further relaxation of the system leads to evolution along an energy plateau (shaded area), where the molecular motion is dominated by torsional deformation about the chemically relevant central double bond. We have proposed that the picosecond FS observed in solution PSB11 corresponds to “slow” evolution along the S_1 energy plateau. Notice that such torsional motion is not impulsive but will be initiated after partial internal vibrational energy redistribution (IVR) from totally symmetric to non totally symmetric modes.

Presently, the quality of the computed potential energy surface and, in turn, the accuracy of the proposed dynamic model have been accessed only through a *qualitative* comparison with absorption, emission, and RR spectroscopic data of solution

PSB11.¹⁰ A further step in the direction of providing a full and consistent understanding of the S_1 potential energy surface of PSB11 is to assess whether the same model accounts for the *details* of the RR spectrum of the visual chromophore in solution and provide indications on the changes that the S_0, S_1 potential energy surfaces must undergo to explain the much shorter time scale dynamics in rhodopsin.

Interestingly, the RR spectra of PSB11 in solution and of rhodopsin are very similar, especially in the structurally sensitive fingerprint region.^{9,11} However, a major difference occurs in the activity of the band observed at ca. 970 cm^{-1} , which is much more intense in rhodopsin.¹¹ This mode was assigned to the out-of-phase 11,12 hydrogen out-of-plane (HOOP) wagging motion,¹² and its activity was interpreted in terms of increased ground-state distortions about the $C_{10}-C_{11}$, $C_{11}=C_{12}$, and $C_{12}-C_{13}$ bonds of the chromophore in rhodopsin.⁹ The assumption of ground-state distortion led to the appealing suggestion of twisting around the $C_{11}=C_{12}$ bond such that the isomerization process would be *primed* in rhodopsin.^{8,9} From the experiments, it is not clear, however, to what extent such twisting should be reduced in free PSB11 in order to account for both the decreased RR activity and the slower dynamics observed in solution.

The simulations based on the ab initio quantum chemical calculations reported in this work provide evidence that the RR spectra of free PSB11 in solution are compatible with an initial *in-plane* relaxation of the chromophore in S_1 , as shown in Figure 1. Here we focus mainly on the motion which describes the acceleration out of the FC point and production of the observed fluorescent state. Several analyses and simulations^{13–17} of RR intensities of retinal chromophores were proposed, based on empirical force field calculations¹⁴ or semiempirical quantum chemical calculations.^{15–17} Ab initio quantum chemical calculations of various properties of protonated Schiff bases have appeared recently,¹⁸ but, to date, this is the first simulation of RR intensities based entirely on ab initio computed molecular parameters. The simulations were performed on a model of PSB11, carefully chosen to contain the most significant mo-

(11) Mathies, R.; Freedman, T. B.; Stryer, L. *J. Mol. Biol.* **1977**, *109*, 367–372.

(12) Eyring, G.; Curry, B.; Broek, A.; Lugtenburg, J.; Mathies, R. *Biochemistry* **1982**, *21*, 384–393.

(13) Eyring, G.; Curry, B.; Mathies, R.; Fransen, R.; Palings, I.; Lugtenburg, J. *Biochemistry* **1980**, *19*, 2410–2418.

(14) (a) Curry, B.; Broek, A.; Lugtenburg, J.; Mathies, R. *J. Am. Chem. Soc.* **1982**, *104*, 5274–5286. (b) Curry, B.; Palings, I.; Broek, A.; Pardoen, J. A.; Mulder, P. P. J.; Lugtenburg, J.; Mathies, R. *J. Phys. Chem.* **1984**, *88*, 688–702. (c) Smith, S. O.; Myers, A. B.; Mathies, R. A.; Pardoen, J. A.; Winkel, C.; van den Berg, E. M. M.; Lugtenburg, J. *Biophys. J.* **1985**, *47*, 653–664. (d) Smith, S. O.; Pardoen, J. A.; Lugtenburg, J.; Mathies, R. A. *J. Phys. Chem.* **1987**, *91*, 804–819. (e) Smith, S. O.; Braiman, M. S.; Myers, A. B.; Pardoen, J. A.; Courtin, J. M. L.; Winkel, C.; Lugtenburg, J.; Mathies, R. A. *J. Am. Chem. Soc.* **1987**, *109*, 3108–3125. (f) Palings, I.; van den Berg, E. M. M.; Lugtenburg, J.; Mathies, R. *Biochemistry* **1989**, *28*, 1498–1507. (g) Ames, J. B.; Fodor, S. P. A.; Gebhard, R.; Raap, J.; van den Berg, E. M. M.; Lugtenburg, J.; Mathies, R. A. *Biochemistry* **1989**, *28*, 3681–3687. (h) Shreve, A. P.; Mathies, R. A. *J. Phys. Chem.* **1995**, *99*, 7285–7299.

(15) (a) Warshel, A.; Karplus, M. *J. Am. Chem. Soc.* **1974**, *96*, 5677–5689. (b) Warshel, A. *Annu. Rev. Biophys. Bioeng.* **1977**, 273–300.

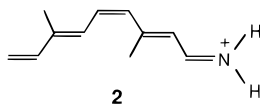
(16) Warshel, A.; Dauber, P. *J. Chem. Phys.* **1977**, *66*, 5477–5488.

(17) Warshel, A.; Barboy, N. *J. Am. Chem. Soc.* **1982**, *104*, 1469–1476.

(18) (a) Deng, H.; Huang, L.; Groesbeek, M.; Lugtenburg, J.; Callender, R. H. *J. Phys. Chem.* **1994**, *98*, 4776–4779. (b) Sakurai, M.; Wada, M.; Inoue, Y.; Tamura, Y.; Watanabe, Y. *J. Phys. Chem.* **1996**, *100*, 1957–1964. (c) Masuda, S.; Torii, H.; Tasumi, M. *J. Phys. Chem.* **1996**, *100*, 15328–15334. (d) Masuda, S.; Torii, H.; Tasumi, M. *J. Phys. Chem.* **1996**, *100*, 15335–15339. (e) Dobado, J. A.; Nonella, M. *J. Phys. Chem.* **1996**, *100*, 18282–18288. (f) Houjou, H.; Sakurai, M.; Asakawa, N.; Inoue, Y.; Tamura, Y. *J. Am. Chem. Soc.* **1996**, *118*, 8904–8915. (g) Bifone, A.; de Groot, H. J. M.; Buda, F. *Pure Appl. Chem.* **1997**, *69*, 2105–2110. (h) Froese, R. D. J.; Komaromi, I.; Byun, K. S.; Morokuma, K. *Chem. Phys. Lett.* **1997**, *272*, 335–340.

(10) Garavelli, M.; Vreven, T.; Celani, P.; Bernardi, F.; Robb, M. A.; Olivucci, M. *J. Am. Chem. Soc.* **1998**, *120*, 1285–1288.

lecular characteristics of the retinal chromophore. At the same time, the size of the model was limited by the computational effort required to perform high-level quantum chemical calculations. To describe as accurately as possible the details of the vibronic structure, especially in the fingerprint region of the RR spectrum, we selected, as PSB11 model, the γ,η -dimethyl analogue (**2**) of the previously investigated PSB11 model **1**.¹⁰



As will be shown, **2** simultaneously accounts for the slower dynamics and the spectroscopy of free PSB11 in solution. In turn, the simulations strongly support the potential energy surface structure presented in Figure 1, which is also further validated via geometry optimization and vibrational frequencies computations along the relaxation path of model **1**. Secondly, but not less importantly, the accuracy of the simulations presented here for PSB11 suggests that the quantum chemical methods employed in this work can be used in the structural characterization of photoreaction intermediates whose spectra have been recently obtained with greatly improved signal-to-noise ratios.^{19,20}

2. Computational Details and Modeling of RR Spectra

The excitation wavelength employed to measure the RR spectrum of PSB11 was in resonance with the singlet electronic excited state S_1 , whose $S_0 \rightarrow S_1$ transition dipole moment is strongly allowed.⁹ As a consequence, the FC mechanism (A term in Albrecht's notation²¹) is the main source of intensity, and the vibrational structure of the RR spectra discussed in the following will be assumed to be dominated by the activity of totally symmetric modes.

To simulate the spectra, we adopted the harmonic approximation and obtained, for each i th totally symmetric mode, the displacement parameters B_i relative to the $S_0 \rightarrow S_1$ transition. The latter are defined as²²

$$B_i = (2.41 \times 10^6) \mathbf{f}^{\mathbf{S}_1} \mathbf{M}^{1/2} \mathbf{L}_i^{\mathbf{S}_0} \nu_i^{-3/2} \quad (1)$$

where $\mathbf{f}^{\mathbf{S}_1}$ is the $3N$ -dimensional Cartesian vector of forces in S_1 (atomic units), \mathbf{M} is the $3N \times 3N$ diagonal matrix of atomic masses, $\mathbf{L}_i^{\mathbf{S}_0}$ is the $3N$ vector describing the normal coordinate $\mathbf{Q}_i^{\mathbf{S}_0}$ in terms of mass-weighted Cartesian coordinates, and ν_i is the associated vibrational frequency (cm^{-1}).

Under the assumption of resonance with the 0–0 band of the $S_0 \rightarrow S_1$ transition, the activity of each totally symmetric mode is related to the displacement parameter through the γ_i parameter:

$$I_i \propto \gamma_i = \frac{1}{2} B_i^2 \quad (2)$$

Thus, to simulate the RR spectra, we need to compute the ground-state equilibrium geometry and vibrational frequencies along with the gradient in the resonant state (S_1) at the equilibrium geometry of the ground state.

All the computations reported in this paper were performed at the ab initio CASSCF level of theory using the 6-31G* basis set available in Gaussian94.²³ The full active space of 10 π electrons in 10 π orbitals (10e/10o) was used for the ground-state optimization of **2**, as well as

to compute its FC excited-state gradient. As a result of this full (unconstrained) optimization, a planar minimum on S_0 was obtained. Due to the impossibility to perform CASSCF/6-31G* 10e/10o analytical frequencies computations on the S_0 -optimized model system, the S_0 vibrational force field was computed on the 10e/10o optimized structure via analytical frequencies computations with a restricted active space of 8 π electrons in 8 π orbitals (8e/8o), by rejecting the almost doubly occupied and almost empty orbitals of the former full active space. On a shorter PSB11 model (2-*cis*-penta-2,4-dieniminium cation), this approach produced results comparable to those obtained with the use of the full active space.

To strengthen the interpretation of the RR spectra in terms of motion along the energy surface of Figure 1, we have evaluated the curvature of the S_1 surface along the relaxation path by performing two large CASSCF/6-31G* 10e/10o numerical frequencies computations on model **1**. The first computation was carried out at a point located along the previously reported S_1 relaxation path¹⁰ and in the vicinity of the FC point (more specifically, this point corresponds to the point placed at 0.5 $\text{amu}^{1/2}$ bohr distance—given in mass-weighted Cartesians—from the FC point in Figure 1 of ref 10). The second computation was carried out at a stationary point (i.e., **SP** in Figure 1) located via a CASSCF/6-31G* 10e/10o geometry optimization and corresponding to the fully relaxed planar S_1 structure. Notice that, since the first point is nonstationary, the surface curvature was evaluated by computing the frequencies along the $(n - 1)$ -dimensional space orthogonal to the direction of the relaxation path (i.e., to the gradient in mass-weighted Cartesians).²⁴

3. Results and Discussion

The positions of the bands in a RR spectrum correspond to vibrational frequencies in the ground state of the chromophore. Their intensities, conversely, contain information on the shape of the excited electronic state since they depend on the geometrical distortion of the molecule upon light absorption. Turning the problem from the computational point of view, the quality of predicted S_0, S_1 potential energy surfaces is reflected in the accuracy of simulated RR intensities. Generally, the prediction of vibrational properties requires a very accurate description of potential energy surfaces. In the simplest approach of molecular mechanics, familiar to most chemists, this is achieved through the inclusion of specific potential terms usually not required to describe satisfactorily equilibrium structures on the energy surfaces. In quantum chemistry, the accuracy is improved by the inclusion of correlation energy, and in our experience the CASSCF level of theory provides a very reliable description of molecular parameters required to simulate the vibronic activity in electronic spectra.^{25,26} In particular, we have recently analyzed the RR spectra of hexatriene in the lowest triplet state²⁶ and found an excellent agreement between simulated and observed spectra.

The vibrational frequencies and the associated γ parameters computed for the PSB11 model **2** are listed in Table 1, while

(23) Frisch, M. J.; Trucks, G. W.; Schlegel, H. B.; Gill, P. M. W.; Johnson, B. G.; Robb, M. A.; Cheeseman, J. R.; Keith, T.; Petersson, G. A.; Montgomery, J. A.; Raghavachari, K.; Al-Laham, M. A.; Zakrzewski, V. G.; Ortiz, J. V.; Foresman, J. B.; Peng, C. Y.; Ayala, P. Y.; Chen, W.; Wong, M. W.; Andres, J. L.; Replogle, E. S.; Gomperts, R.; Martin, R. L.; Fox, D. J.; Binkley, J. S.; Defrees, D. J.; Baker, J.; Stewart, J. P.; Head-Gordon, M.; Gonzalez, C.; Pople, J. A. *Gaussian 94, Revision B.2*; Gaussian, Inc.: Pittsburgh, PA, 1995.

(24) The vibrational frequencies at nonstationary points (i.e., points with a nonzero energy gradient, such as the MEP points) are obtained from the computed Hessian by projection onto the $(n - 1)$ -dimensional space orthogonal to the gradient. See: (a) Miller, W. H.; Handy, N. C.; Adams, J. E. *J. Chem. Phys.* **1980**, *72*, 99–112 (b) Truhlar, D. G.; Gordon, M. S. *Science* **1990**, *249*, 491–498.

(25) (a) Negri, F.; Zgierski, M. Z. *J. Chem. Phys.* **1993**, *99*, 4318–4326. (b) Negri, F.; Zgierski, M. Z. *J. Chem. Phys.* **1995**, *102*, 5165–5173.

(26) (a) Negri, F.; Orlandi, G. *J. Chem. Phys.* **1995**, *103*, 2412–2419. (b) Negri, F.; Orlandi, G. *J. Photochem. Photobiol. A: Chem.* **1997**, *105*, 209–216.

(19) Jager, F.; Ujj, L.; Atkinson, G. H. *J. Am. Chem. Soc.* **1997**, *119*, 12610–12618.

(20) Jager, F.; Lou, J.; Nakanishi, K.; Ujj, L.; Atkinson, G. H. *J. Am. Chem. Soc.* **1998**, *120*, 3739–3747.

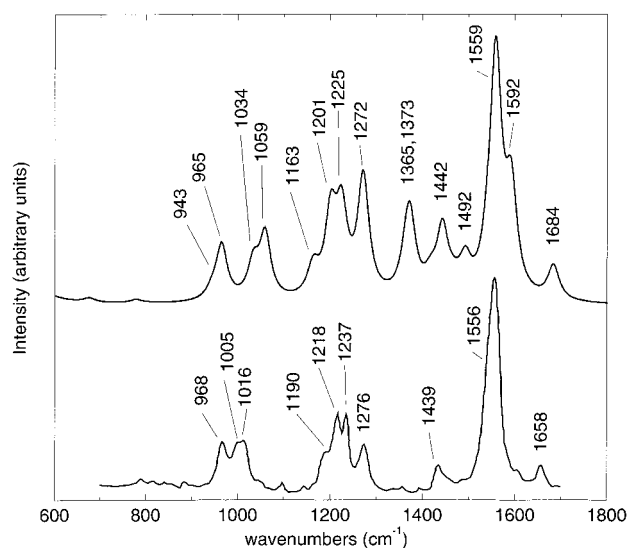
(21) (a) Albrecht, A. C. *J. Chem. Phys.* **1961**, *34*, 1476–1484. (b) Clark, R. J. H.; Dines, T. *J. Angew. Chem., Int. Ed. Engl.* **1986**, *25*, 131–158.

(22) ten Wolde, A.; Jacobs, H. J. C.; Langkilde, F. W.; Bajdor, K.; Wilbrandt, R.; Negri, F.; Zerbetto, F.; Orlandi, G. *J. Phys. Chem.* **1994**, *98*, 9437–9445.

Table 1. Computed Vibrational Frequencies (*CH* Stretchings not Included) of 4-*cis*- γ , η -Dimethyl-C₉H₉NH₂⁺ (PSB11 Model 2) and γ Parameters Employed to Simulate the RR Spectrum

in-plane				out-of-plane	
ν^a	ν^b	γ	exp ^c	ν^a	ν^b
1871	1684	0.04	1658	1630	1467
1769	1592	0.11	1556	1624	1462
1763	1587	0.01		1187	1068
1732	1559	0.26	1556	1141	1027
1712	1541	0.03		1134	1021
1658	1492	0.03		1039	935
1644	1480			1034	931
1628	1465	0.01		937	843
1603	1442	0.07	1439	904	814
1581	1423			891	802
1574	1417	0.01		832	749
1562	1406			807	726
1526	1373	0.07		735	662
1517	1365	0.03		681	613
1513	1362	0.01		594	535
1431	1288			434	391
1413	1272	0.13	1276	389	350
1361	1225	0.09	1237	276	248
1335	1201	0.09	1218	235	212
1293	1163	0.03	1190	199	179
1186	1067			169	152
1177	1059	0.07	1016	158	142
1149	1034	0.04	1005	87	78
1072	965	0.06	968	34	31
1048	943	0.01		20	18
894	805				
865	779				
751	676				
606	565	0.06			
537	483	0.24			
482	434	0.14			
445	400	0.03			
347	312				
328	295	0.05			
243	219	0.08			
189	170	0.60			
89	80	0.02			

^a CASSCF/6-31G* 8e/8o // CASSCF/6-31G* 10e/10o vibrational frequencies (see also section 2). ^b Scaled uniformly by 0.9. ^c Bands observed in the RR of PSB11 in solution, from ref 11.

**Figure 2.** Comparison of experimental (bottom) and simulated (top) resonance Raman spectrum of PSB11.

the simulated RR spectrum is depicted in Figure 2, where it is compared with the spectrum of PSB11 in solution taken from ref 11. A Lorentzian line width of 15 cm⁻¹ was used to plot the

computed spectrum. The similarity between simulated and observed spectra is striking and suggests that the PSB11 model chosen to mimic the visual chromophore gives a realistic picture of the *S*₀,*S*₁ potential energy changes in PSB11. Indeed, model 2 includes the most important part of the carbon skeleton of retinal. In addition, the two methyl groups, in the same positions as in PSB11, with respect to the *cis* bond, ensure that hindrance effects along with couplings between the polyenic framework and C-CH₃ moieties are also accounted for. However, because of the computational effort required by CASSCF calculations, our molecular model does not include the *n*-butyl group attached to nitrogen and the β -ionone group at the opposite end of the conjugated chain. The rationale behind this choice, apart from computational requirements, is that excitation to *S*₁ affects dominantly the central part of the conjugated structure of the visual chromophore, and the major molecular distortions upon excitation are expected to be accurately described by our PSB11 model. Nevertheless, we are aware that the presence of NH₂- and CH₂-terminal moieties might lead to unrealistic mixing of vibrational normal modes localized on the carbon skeleton with XH₂ (*X* = C, N) rocking and scissoring motions. To establish the influence of this effect on the simulations of RR spectra, we inspected the computed vibrational normal coordinates and identified the vibrations dominated by XH₂ rocking and scissoring motions. The analysis shows that NH₂ and CH₂ scissoring modes mix with CC and CN stretching motions in the frequency region above 1400 cm⁻¹. Inspection of Figure 2 shows, however, that the intensity distribution is correctly predicted in this spectral region: the bands computed at 1442, 1559, and 1684 cm⁻¹ are readily assigned to those observed at 1439, 1556, and 1658 cm⁻¹, respectively. The only notable effect of mixing with NH₂ scissoring is the overestimate of the 1684 cm⁻¹ frequency, compared to the observed 1658 cm⁻¹ value.¹¹ Similarly, the overestimate of the band at 1592 cm⁻¹ can be attributed to mixing with the CH₂ scissoring. Interestingly, the presence of two predicted bands in the 1560–1590-cm⁻¹ region of our simulations is consistent with very recent PR/CARS measurements on rhodopsin,¹⁹ in which two bands were identified, at 1536 and 1548 cm⁻¹, respectively. Notice that, in ref 19, the first of the two bands is less intense than the second. Our simulations predict the opposite as a result of coupling with the CH₂ scissoring motion, which pushes the less intense band to higher frequencies (at 1592 cm⁻¹). In summary, the high-frequency region of the RR spectrum of PSB11 is well reproduced by the simulations, in terms of both band position and intensities. The intensity overestimate at ca. 1370 cm⁻¹ appears to be due to the imperfect balance (at CASSCF level) of CC and CN stretching contributions to the normal coordinate associated with this frequency. Indeed, the intensity in this frequency region decreases when vibrational normal coordinates computed with density functional theory (DFT)²⁷ are employed (see Supporting Information).

Although considerable intensity appears in the high-frequency region, significantly more important is the structurally sensitive fingerprint region (1100–1300 cm⁻¹) of the RR spectrum. Inspection of the normal coordinates associated with frequencies covering this region shows that these are not mixed with XH₂ motions. This is an important result because the activity in this frequency region identifies the isomeric form of the chro-

(27) Vibrational frequencies and normal coordinates were computed at the B3LYP/6-31G* level of theory at the CASSCF/6-31G* 10e/10o ground-state geometry. Generally, DFT frequencies compare very well with experimental data. In the present case, however, the force field was evaluated at the CASSCF/6-31G* 10e/10o equilibrium geometry since B3LYP/6-31G* geometry is less satisfactory. This resulted in generally less reliable vibrational frequencies compared to the CASSCF set discussed in the text.

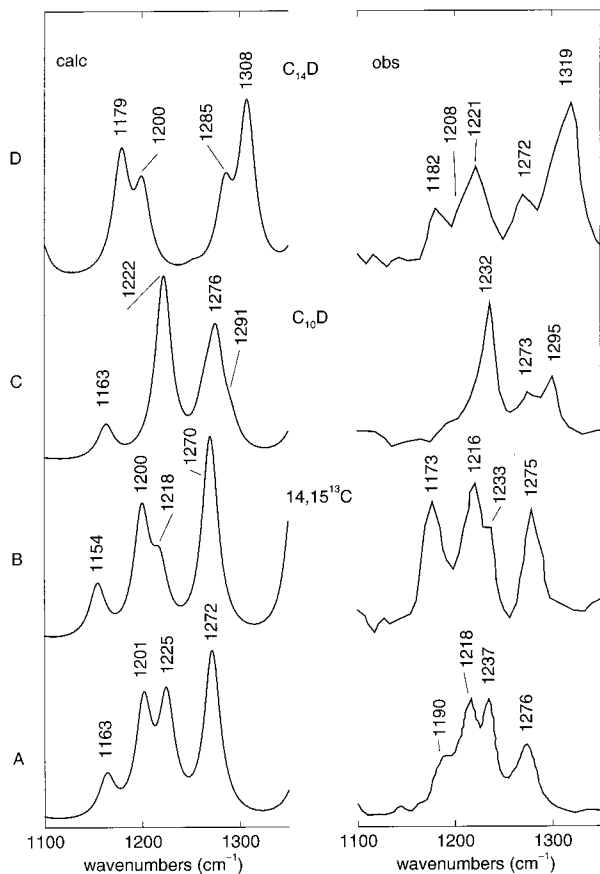


Figure 3. Comparison of simulated (left) and observed (right) RR spectra of PSB11 and its isotopomers: (A) PSB11 model 2; (B) $^{13}\text{C}_{14}, ^{13}\text{C}_{15}$; (C) C_{10}D ; (D) C_{14}D . Carbon atom numbering according to the PSB11 given above.

mophore, and the absence of perturbations due to the truncated size of the molecular model employed in the calculations ensures that the PSB11 model can be used also to predict spectral changes due to structural changes of the chromophore, such as those occurring during the formation of photoreaction intermediates. Four main bands were observed in the RR spectrum of PSB11 in solution and in rhodopsin,^{8,9,11} at 1190, 1218, 1237, and 1276 cm^{-1} , and four bands are correspondingly predicted in the RR spectrum of our model PSB11, at 1163, 1201, 1225, and 1272 cm^{-1} , with intensities very similar to those observed. The accuracy of these predictions can be additionally proved by simulating the RR spectra of some isotopomers of PSB11. In Figure 3, the simulations of the RR spectra of the $^{13}\text{C}_{14}, ^{13}\text{C}_{15}$ -, C_{10}D -, and C_{14}D - isotopomers are compared with the spectrum of the isotopically unsubstituted model of PSB11. Similarly, the spectra of the $^{13}\text{C}_9$ -, $^{13}\text{C}_{10}, ^{13}\text{C}_{11}$ -, and $^{13}\text{C}_{13}$ - isotopomers are presented in Figure 4, and those of the C_{11}D -, C_{12}D -, C_{15}D -, and $\text{C}_{11}\text{D}, \text{C}_{12}\text{D}$ - isotopomers are depicted in Figure 5. For the sake of simplicity, the carbon atom numbering chosen to label the isotopic substitutions corresponds to the PSB11 molecule. The simulations in Figures 3 and 4 are compared with the experimental spectra of PSB11 in solution,⁹ while the spectra in Figure 5 are compared with those of rhodopsin.¹² Although there are differences between the RR spectra of PSB11 in solution and in the protein, these do not concern the fingerprint region. In this sense, the comparison of simulated spectra with those of rhodopsin (see Figure 5) is meaningful if limited to this spectral region. Inspection of the spectra in Figures 3–5 shows that the effects of isotopic substitution are well reproduced by the calculations. This leaves

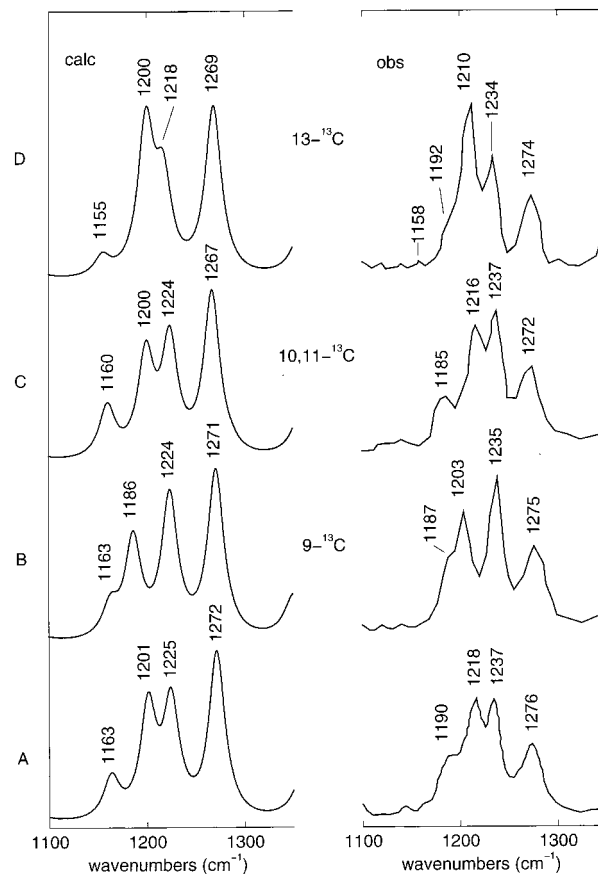


Figure 4. Comparison of simulated (left) and observed (right) RR spectra of PSB11 and its isotopomers: (A) PSB11 model 2; (B) $^{13}\text{C}_9$; (C) $^{13}\text{C}_{10}, ^{13}\text{C}_{11}$; (D) $^{13}\text{C}_{13}$. Carbon atom numbering according to the PSB11 given above.

little doubt about the quality of the calculations and the representativeness of the molecular model to describe PSB11.

There is, however, another interesting region in the RR spectra of PSB11, between 900 and 1100 cm^{-1} . The activity in this frequency region discriminates between PSB11 in solution and rhodopsin and is considered to be important to establish the effect of protein environment on the chromophore, since similar bands are observed but with remarkably different intensities for the two systems. The band observed at 970 cm^{-1} shows a dramatic intensity increase when going from PSB11 in solution to rhodopsin. According to deuteration effects,¹² most of the intensity of this band was attributed to the out-of-phase $\text{C}_{11}\text{H}, \text{C}_{12}\text{H}$ HOOP wagging motion of the chromophore. Since this is the motion hydrogens must follow when the double bond undergoes *cis* \rightarrow *trans* isomerization, the strong activity of this band suggested a mechanism of initial relaxation on the S_1 state of rhodopsin *in the direction required by the torsional motion*. Turning now to free PSB11 in solution, the weaker intensity of the 970- cm^{-1} band suggests a much smaller driving force in the direction of the *CH* wagging motion and, consequently, along the torsional movement of the chromophore. However, the extent of reduction of potential energy distortion consistent with the observed RR activity has not been established. As anticipated in the previous section, the CASSCF calculations performed on models 1 and 2 predict a planar equilibrium structure in S_0 which, combined with the computed structure of the S_1 energy surface (see Figure 1), indicates that the initial relaxation occurs along in-plane (i.e., totally symmetric) modes. This might appear to be inconsistent with the activity observed around 970 cm^{-1} in the RR spectra of free PSB11 in solution.

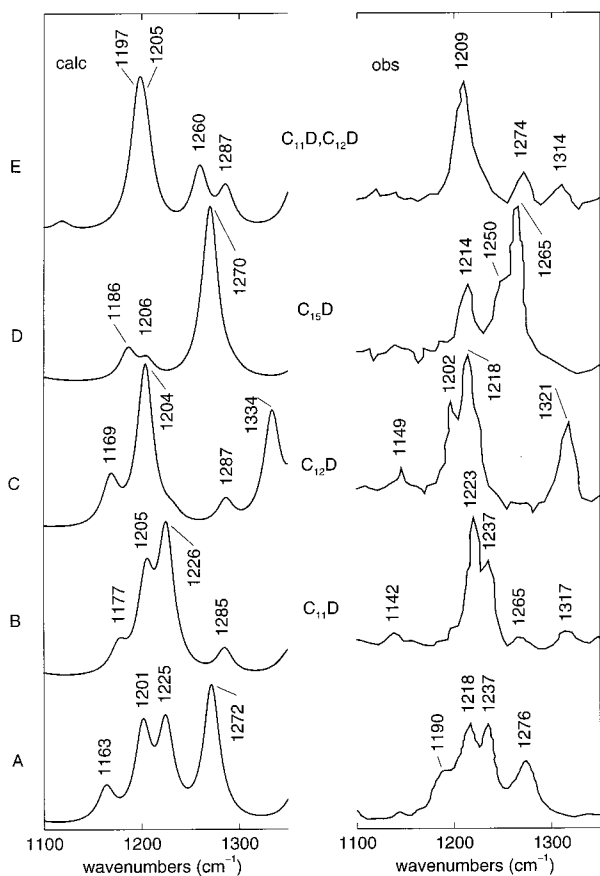


Figure 5. Comparison of simulated (left) and observed (right) RR spectra of PSB11 and its isotopomers: (A) PSB11 model 2; (B) $C_{11}D$; (C) $C_{12}D$; (D) $C_{15}D$; (E) $C_{11}D, C_{12}D$. Carbon atom numbering according to the PSB11 given above.

Conversely, our simulations reproduce correctly the experimental spectra and lead us to the conclusion that the observed activity is due *only* to in-plane relaxation of the chromophore. Indeed, inspection of the simulated RR spectrum for **2** (see Table 1 and Figure 2) reveals that the bands, due to in-plane modes, computed at 965, 1034, and 1059 cm^{-1} ²⁸ can be assigned to the bands observed at 968, 1005, and 1016 cm^{-1} ,¹¹ respectively. The out-of-phase $C_{11}H, C_{12}H$ HOOP wagging vibration falls in the *same frequency region* (our calculations predict it at 931 cm^{-1} , but this value might be underestimated) but, according to our model, is RR inactive in isolated PSB11. On the contrary, this mode is certainly responsible for the increased activity at 970 cm^{-1} in rhodopsin, where both in-plane and out-of-plane modes contribute to the total intensity.

The simulation and analysis of RR activities of PSB11 in solution discussed in this work combined with the dynamical model proposed in ref 10 support the hypothesis that the energy surface in Figure 1 provides a correct representation of the force field controlling the excited-state motion of PSB11 in solution. Accordingly, the chromophore must accelerate along a totally symmetric coordinate until a fully relaxed planar structure is reached. This model holds only if the initial relaxation path (see Figure 1) develops along a *valley-shaped* potential energy region which prevents the spreading of the initially prepared vibrational

(28) At variance with the vibrations of the structurally sensitive fingerprint region, the vibrational normal coordinates falling in the 900–1100- cm^{-1} frequency region are perturbed by mixing with XH_2 ($X = C, N$) rocking vibrations. However, we have verified that the effect of terminal hydrogen motion does not affect the RR activities. These reflect the S_0, S_1 geometry change of the chromophore and are not contaminated by effects of truncations due to the size of the model PSB11.

wave packet. To confirm the existence of such a region, we have computed the vibrational frequencies (see section 2) at point SP and at a point close to FC, as these points are located at the end and at the beginning of the relaxation path, respectively. Since the resulting vibrational frequencies are all real, the computations confirm the valley-shaped nature of the S_1 surface in this region. However, while the planar structure SP corresponds to a local minimum on the S_1 energy surface, there are at least two low-frequency modes, whose frequencies are computed at 254 and 359 cm^{-1} , involving *cis* \rightarrow *trans* isomerization motion, which suggests a facile torsional deformation. Indeed, the deformation of SP along these modes and, in particular, along the central bond torsional coordinate does not change the energy significantly, suggesting a highly anharmonic behavior. In fact, a 5° rotation about the central bond changes the energy of the system by less than 0.1 kcal mol^{-1} . In contrast, near the FC point, the same rotation leads to a 2.5 kcal mol^{-1} energy *increase*, which indicates a well-defined valley. This surface structure is also consistent with the fact that the central bond lengths of the SP and FC structures are 1.48 and 1.36 Å, respectively. The same type of excited-state structure has been documented for the *all-trans*-hepta-2,4,6-trieniminium cation,²⁹ a shorter model (four conjugating double bonds) of the PSBT isomer.

The conclusion that Figure 1 provides a correct representation of the force field for PSB11 in solution implies that the chromophore does not strongly interact with the counterion (usually a chlorine or a trichloroacetate anion) and is present as a solvent-separated ion pair. The absence of out-of-plane motion in the initial dynamics of the photoexcited system implies that the transient picosecond FS is generated by femtosecond skeletal relaxation followed by energy redistribution to out-of-plane modes (see the trajectory depicted in Figure 1). The time scales for depopulation of the FC region and excited-state dynamics have been recently measured by Zinth et al.³⁰ for the PSBT isomer in methanol solution using femtosecond absorption spectroscopy. This process is assigned to a ca. 100-fs transient signal, which is then followed by slower nonexponential decay with 2.0- and 7.0-ps time constants which correspond to the FS observed by Kandori and Sasabe.³¹ This behavior seems to be general for retinal protonated Schiff bases in solution. In fact, similar time scales have been reported by Kandori et al.³ for PSB11 and by El-Sayed et al.³² for the 13-*cis* isomer. We assign the 100-fs process to the in-plane skeletal motion along the valley shown in Figure 1.

To provide an estimate of the time scale required for the initial motion out of the FC region, we have used the multidimensional separable harmonic surface model (formula 50 in ref 33) and the force field defined by the vibrational frequencies at SP to simulate the excited state motion along the totally symmetric subspace (47 modes) of **1**. The validity of this approximation is supported by the quality of the simulated RR spectra, which indicates harmonic totally symmetric modes. The simulation shows that a trajectory released at FC with no initial kinetic energy reaches the bottom of the valley in 10 fs and that the first oscillation of the central bond is completed in 26 fs and

(29) Garavelli, M.; Bernardi, F.; Olivucci, M.; Vreven, T.; Klein, S.; Celani, P.; Robb, M. A. *Faraday Discuss.* **1998**, *110*, 51–70.

(30) Hamm, P.; Zurek, M.; Röschinger, T.; Patzelt, H.; Oesterheld, D.; Zinth, W. *Chem. Phys. Lett.* **1996**, *263*, 613–621.

(31) Kandori, H.; Sasabe, H. *Chem. Phys. Lett.* **1993**, *16*, 126–132.

(32) Logunov, S. L.; Song, L.; El-Sayed, M. A. *J. Phys. Chem.* **1996**, *100*, 18586–18591.

(33) Myers, A. B.; Mathies, R. A. in *Biological Application of Raman Spectroscopy*, Vol. 2; Spiro, T. G., Ed.; Wiley-Interscience: New York, 1987; pp 1–58.

the second, third, and fourth in 44, 62, and 86 fs, respectively. This estimate indicates that, during the observed 100-fs process, the molecule shall carry out 3–4 oscillations before being displaced along the out-of-plane (i.e., torsional) modes.

The following picosecond process (which corresponds to the FS dynamics) is instead assigned to IVR and evolution along the subsequent flat energy plateau. As previously reported,¹⁰ our computations cannot exclude the existence of a small barrier along the plateau. Indeed, a 600-cm⁻¹ barrier has been recently reported for PSBT in solution.

The RR spectra indicate that, in rhodopsin, the chromophore will initially accelerate along the same stretching and bending modes which describe relaxation in a solution environment. Interestingly, a very recent resonance Raman study of the excited state of bacteriorhodopsin³⁴ provides experimental evidence that also the initial relaxation of its PSBT chromophore involves skeletal stretching motion. Furthermore, the evidence for only a limited contribution of the chromophore torsional deformation on the initial dynamics of rhodopsin came from the recent analysis of deuterium substitution effects on the Fourier transform of the optical absorption spectra.³⁵ Nevertheless, the RR spectrum of rhodopsin clearly indicates out-of-plane and, specifically, torsional mode activity,^{8,36} which suggests that the rhodopsin chromophore is nonplanar and that skeletal relaxation may be coupled with out-of-plane deformations. In fact, one expects that the “asymmetric” rhodopsin cavity could stabilize a moderately twisted ground-state chromophore. Indeed, a protein cavity with a strategically placed counterion³⁷ could change the shape of the entire S_0 and S_1 energy surfaces, break their torsional symmetry, remove the energy plateau on S_1 , and lead to a faster excited-state dynamics.

This idea is partly supported by the recently reported result of ab initio semiclassical trajectory computations of the 1-methyl-2-*cis*-penta-2,4-dieniminium cation, a minimal PSB11 model.^{38,39} Like models **1** and **2**, this molecule is planar and has a symmetric S_1 energy surface. However, the corresponding S_1 relaxation path is fully barrierless and does not show an energy plateau. The limited size of this model has allowed for the investigation of the excited-state dynamics by computing few semiclassical trajectories starting from slightly twisted structures. The results indicate an excited-state lifetime of ca. 20–40 fs,³⁹ closer to that observed for PSB11 in rhodopsin than that in solution.

4. Conclusions

A model describing the evolution of PSB11 on its lowest excited state and the effect of the protein environment must

(34) Song, L.; El-Sayed, M. A. *J. Am. Chem. Soc.* **1998**, *120*, 8889–8890.

(35) Kakitani, T.; Akiyama, R.; Hatano, Y.; Yamamoto, Y.; Shichida, Y.; Verdegem, P.; Lugtenburg, J. *J. Phys. Chem. B* **1998**, *102*, 1334–1339.

(36) Lin, S. W.; Groesbeek, M.; van der Hoef, I.; Verdegem, P.; Lugtenburg, J.; Mathies, R. A. *J. Phys. Chem. B* **1998**, *102*, 2787–2806.

(37) (a) Han, M.; Smith, M. *Biophys. Chem.* **1995**, *56*, 23–29. (b) Han, M.; DeDecker, B. S.; Smith, M. *Biophys. J.* **1993**, *65*, 899–906.

(38) Garavelli, M.; Celani, P.; Bernardi, F.; Robb M. A.; Olivucci, M. *J. Am. Chem. Soc.* **1997**, *119*, 6891–6901.

(39) Vreven, T.; Bernardi, F.; Garavelli, M.; Olivucci, M.; Robb, M. A.; Schlegel, H. B. *J. Am. Chem. Soc.* **1997**, *119*, 12687–12688.

account simultaneously for the combined results of RR and femtosecond spectroscopic studies. In this work, we have concentrated on the first of the two experimental sources of information. Accordingly, the resonance Raman spectra of PSB11 and several isotopic derivatives have been simulated by performing high-level quantum chemical calculations on 4-*cis*- γ,η -dimethyl-C₉H₉NH₂⁺ (i.e., model **2**), a computationally manageable and “realistic” model of PSB11. The comparison between the simulated and experimental spectra of PSB11 in solution reveals a very close agreement. The RR response in the structurally sensitive fingerprint region of the spectrum is reproduced accurately for PSB11 and its isotopomers. This implies that the method can be employed quantitatively to assist in the characterization of photoreaction intermediates in the visual cycle. Remarkably, the simulations also reproduce the activity observed in the RR spectrum of PSB11 in solution at ca. 970 cm⁻¹. This result strongly suggests that only in-plane motions contribute in this region, in contrast with rhodopsin, where a superposition of in-plane and out-of-plane motions is responsible for the dramatically increased activity.

The lack of acceleration along out-of-plane modes in the initial relaxation out of the FC region of PSB11 in solution, emerging from the analysis of RR intensities based on simulated spectra and from the characterization of the initial relaxation path performed in this study, is consistent with the previously proposed photoisomerization model characterized by initial skeletal relaxation followed by slow evolution along a plateau on the torsional subspace of the S_1 potential energy surface. In this sense, the scheme proposed on the basis of high-level ab initio quantum chemical calculations on the realistic PSB11 model accounts for both the spectroscopy and the time scale of photoisomerization dynamics of PSB11 in solution.

Acknowledgment. This research has been supported by the University of Bologna (Funds for selected research topics: Project “Materiali innovativi”), by CNR (Project “Applicazioni di spettroscopie ottiche”), and by an EU TMR network grant (ERB 4061 PL95 1290, Quantum Chemistry for the Excited State). M.O. is also grateful to NATO for a travel grant (CRG 950748).

Supporting Information Available: Tables containing the computed ground-state equilibrium structure of 4-*cis*- γ,η -dimethyl-C₉H₉NH₂⁺, the computed fully relaxed planar S_1 state structure of 4-*cis*- γ -methyl-C₉H₉NH₂⁺, the vibrational frequencies and γ parameters (RR intensities) computed for the isotopomers of the PSB11 model discussed in this work, the comparison between computed and observed isotopic shifts in the structurally sensitive fingerprint region, and B3LYP/6-31G* vibrational frequencies and γ parameters (RR intensities) for isotopically unsubstituted model PSB11 (PDF). See any current masthead page for ordering information and Web access instructions.

JA981719Y